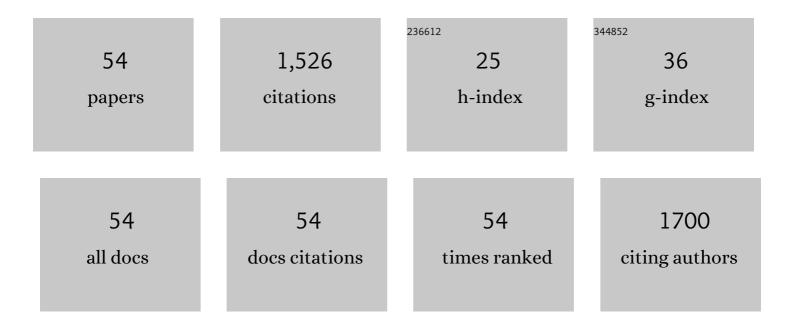
Zhong Liu

List of Publications by Year in descending order

Source: https://exaly.com/author-pdf/5807992/publications.pdf Version: 2024-02-01



7номс Ци

#	Article	IF	CITATIONS
1	Dendritic fibrous nano-particles (DFNPs): rising stars of mesoporous materials. Journal of Materials Chemistry A, 2019, 7, 5111-5152.	5.2	103
2	A glassy carbon electrode modified with N-doped carbon dots for improved detection of hydrogen peroxide and paracetamol. Mikrochimica Acta, 2018, 185, 87.	2.5	80
3	Highly efficient oxidative desulfurization of dibenzothiophene using Ni modified MoO3 catalyst. Applied Catalysis A: General, 2020, 589, 117308.	2.2	73
4	Design and facile one-step synthesis of FeWO4/Fe2O3 di-modified WO3 with super high photocatalytic activity toward degradation of quasi-phenothiazine dyes. Applied Catalysis B: Environmental, 2018, 221, 169-178.	10.8	72
5	Corrosion resistance and wetting properties of silica-based superhydrophobic coatings on AZ31B Mg alloy surfaces. Applied Surface Science, 2018, 453, 1-10.	3.1	72
6	Experimental and theoretical investigations of Cs+ adsorption on crown ethers modified magnetic adsorbent. Journal of Hazardous Materials, 2019, 371, 712-720.	6.5	66
7	The adsorption behavior and mechanism of Cr(VI) on 3D hierarchical α-Fe 2 O 3 structures exposed by (0) Tj E	[Qq110.78	84314 rgBT 61
8	(001) plan manipulation of α-Fe2O3 nanostructures for enhanced electrochemical Cr(VI) sensing. Journal of Electroanalytical Chemistry, 2019, 841, 142-147.	1.9	56
9	The polymeric nanofilm of triazinedithiolsilane fabricated by self-assembled technique on copper surface. Part 2: Characterization of composition and morphology. Applied Surface Science, 2015, 356, 191-202.	3.1	54
10	Enhancing the Li+ adsorption and anti-dissolution properties of Li1.6Mn1.6O4 with Fe, Co doped. Hydrometallurgy, 2020, 193, 105291.	1.8	43
11	A solid-state electrochemical sensing platform based on a supramolecular hydrogel. Sensors and Actuators B: Chemical, 2018, 262, 326-333.	4.0	41
12	The polymeric nanofilm of triazinedithiolsilane fabricated by self-assembled technique on copper surface. Part 1: Design route and corrosion resistance. Corrosion Science, 2015, 98, 382-390.	3.0	37
13	Hexagonal α-Fe2O3 nanorods bound by high-index facets as high-performance electrochemical sensor. Journal of Materials Chemistry A, 2013, 1, 3040.	5.2	36
14	Template-free synthesis of mesoporous ^ĵ a-alumina with tunable structural properties. Ceramics International, 2016, 42, 4072-4079.	2.3	35
15	The performance and mechanism of recovering lithium on H4Ti5O12 adsorbents influenced by (1 1 0) and (1 1 1) facets exposed. Chemical Engineering Journal, 2021, 414, 128729.	6.6	35
16	Magnetic and electrochemical behavior of rhombohedral α-Fe2O3 nanoparticles with (1 0 4) dominant facets. Particuology, 2013, 11, 327-333.	2.0	32
17	Hydrothermal preparation of reduced graphene oxide–silver nanocomposite using Plectranthus amboinicus leaf extract and its electrochemical performance. Enzyme and Microbial Technology, 2016, 95, 112-117.	1.6	32
18	Preparation of α-Fe ₂ O ₃ hollow spheres, nanotubes, nanoplates and nanorings as highly efficient Cr(<scp>vi</scp>) adsorbents. RSC Advances, 2016, 6, 82854-82861.	1.7	30

Zhong Liu

#	Article	IF	CITATIONS
19	CO adsorption, dissociation and coupling formation mechanisms on Fe2C(001) surface. Applied Surface Science, 2018, 434, 464-472.	3.1	29
20	Extraction of lithium from salt lake brines by granulated adsorbents. Colloids and Surfaces A: Physicochemical and Engineering Aspects, 2021, 628, 127256.	2.3	29
21	Morphology and magnetic properties of α-Fe2O3 particles prepared by octadecylamine-assisted hydrothermal method. Particuology, 2012, 10, 456-461.	2.0	28
22	Controllable synthesis of mesoporous alumina with large surface area for high and fast fluoride removal. Ceramics International, 2016, 42, 15253-15260.	2.3	28
23	K-gradient doping to stabilize the spinel structure of Li _{1.6} Mn _{1.6} O ₄ for Li ⁺ recovery. Dalton Transactions, 2020, 49, 10939-10948.	1.6	27
24	Fast production of \hat{l}^2 -Ni(OH)2 nanostructures with (001) and (100) plane exposure and their electrochemical properties. Journal of Materials Chemistry A, 2013, 1, 5695.	5.2	26
25	Highly Lithium Adsorption Capacities of H _{1.6} Mn _{1.6} O ₄ Ion‧ieve by Ordered Array Structure. ChemistrySelect, 2019, 4, 10157-10163.	0.7	26
26	Trace doping by fluoride and sulfur to enhance adsorption capacity of manganese oxides for lithium recovery. Materials and Design, 2020, 194, 108867.	3.3	25
27	Removal of Fluoride by Graphene Oxide/Alumina Nanocomposite: Adsorbent Preparation, Characterization, Adsorption Performance and Mechanisms. ChemistrySelect, 2020, 5, 1818-1828.	0.7	23
28	Enabling highly structure stability and adsorption performances of Li1.6Mn1.6O4 by Al-gradient surface doping. Separation and Purification Technology, 2021, 264, 118433.	3.9	22
29	Preparation and Properties of Octadecahedral αâ€Fe ₂ O ₃ Nanoparticles Enclosed by {104} and {112} Facets. European Journal of Inorganic Chemistry, 2012, 2012, 4076-4081.	1.0	21
30	Multi-Walled Carbon Nanotube-Assisted Electrodeposition of Silver Dendrite Coating as a Catalytic Film. Coatings, 2017, 7, 232.	1.2	18
31	Synthesis of granulated Li/Al-LDHs adsorbent and application for recovery of Li from synthetic and real salt lake brines. Hydrometallurgy, 2022, 209, 105828.	1.8	18
32	A rapid electrochemical sensor fabricated using silver ions and graphene oxide. lonics, 2018, 24, 2821-2827.	1.2	17
33	Precisely tailoring dendritic α-Fe2O3 structures along [101̄0] directions. CrystEngComm, 2012, 14, 4074.	1.3	16
34	A multifunctional polymeric nanofilm with robust chemical performances for special wettability. Nanoscale, 2016, 8, 5153-5161.	2.8	16
35	Bubble-template synthesis of WO ₃ ·0.5H ₂ O hollow spheres as a high-activity catalyst for catalytic oxidation of benzyl alcohol to benzaldehyde. CrystEngComm, 2019, 21, 1026-1033.	1.3	15
36	Surface trace doping of Na enhancing structure stability and adsorption properties of Li1.6Mn1.6O4 for Li+ recovery. Separation and Purification Technology, 2021, 256, 117583.	3.9	15

ZHONG LIU

#	Article	IF	CITATIONS
37	A novel method for removal of boron from aqueous solution using sodium dodecyl benzene sulfonate and d-mannitol as the collector. Desalination, 2018, 431, 47-55.	4.0	14
38	Preparation of MnO2–Al2O3 adsorbent with large specific surface area for fluoride removal. Particuology, 2016, 27, 66-71.	2.0	13
39	RF magnetron sputtering synthesis of carbon fibers/ZnO coaxial nanocable microelectrode for electrochemical sensing of ascorbic acid. Materials Letters, 2016, 181, 265-267.	1.3	13
40	Synthesis of FeAPO-5 molecular sieves with high iron contents via improved ionothermal method and their catalytic performances in phenol hydroxylation. Journal of Porous Materials, 2018, 25, 1007-1016.	1.3	13
41	The adsorption behavior of lithium on spinel titanium oxide nanosheets with exposed (1â^'14) high-index facets. Dalton Transactions, 2020, 49, 14180-14190.	1.6	12
42	The role of surface hydrolysis of ferricyanide anions in crystal growth of snowflake-shaped α-Fe ₂ O ₃ . Chemical Communications, 2015, 51, 9350-9353.	2.2	11
43	Synthesis of H ₄ Mn ₅ O ₁₂ Nanotubes Lithium Ion Sieve and Its Adsorption Properties for Li ⁺ from Aqueous Solution. ChemistrySelect, 2019, 4, 9562-9569.	0.7	11
44	Improve the durability of lithium adsorbent Li/Al-LDHs by Fe3+ substitution and nanocomposite of FeOOH. Minerals Engineering, 2022, 185, 107717.	1.8	11
45	Manganese-based spinel adsorbents for lithium recovery from aqueous solutions by electrochemical technique. Journal of Industrial and Engineering Chemistry, 2022, 114, 142-150.	2.9	11
46	Al-doped H ₂ TiO ₃ ion sieve with enhanced Li ⁺ adsorption performance. RSC Advances, 2021, 11, 34988-34995.	1.7	10
47	Fe containing MoO ₃ nanowires grown along the [110] direction and their fast selective adsorption of quasi-phenothiazine dyes. CrystEngComm, 2019, 21, 5106-5114.	1.3	9
48	Chemical conversion based on the crystal facet effect of transition metal oxides and construction methods for sharp-faced nanocrystals. Chemical Communications, 2022, 58, 908-924.	2.2	9
49	Influence of the pH in Reactions of Boric Acid/Borax with Simple Hydroxyl Compounds: Investigation by Raman Spectroscopy and DFT Calculations. ChemistrySelect, 2019, 4, 14132-14139.	0.7	8
50	Hydrothermal synthesis and adsorption behavior of H ₄ Ti ₅ O ₁₂ nanorods along [100] as lithium ion-sieves. RSC Advances, 2020, 10, 35153-35163.	1.7	8
51	A Durable PVDF/PFOTES-SiO2 Superhydrophobic Coating on AZ31B Mg Alloy with Enhanced Abrasion Resistance Performance and Anti-Corrosion Properties. Applied Sciences (Switzerland), 2021, 11, 11172.	1.3	6
52	High Coverage CO Adsorption on Fe6O6 Cluster Using GGA + U. Journal of Cluster Science, 2020, 31, 591-600.	1.7	5
53	The polymeric nanofilm of triazinedithiolsilane capable of resisting corrosion and serving as an activated interface on a copper surface. RSC Advances, 2016, 6, 6811-6822.	1.7	3
54	Facile Synthesis of (110)â€Planeâ€Exposed Au Microflowers as High Sensitive Hydrogen Peroxide Sensors. European Journal of Inorganic Chemistry, 2015, 2015, 2528-2533.	1.0	2